2018

In-Situ Calibration of Underwater Membrane Inlet Mass Spectrometer for Simple Dissolved Gases

Samuel Gartzman
University of Rhode Island, sgartzman@uri.edu

IN-SITU CALIBRATION OF UNDERWATER MEMBRANE INLET MASS SPECTROMETER FOR SIMPLE DISSOLVED GASES

BY

SAMUEL GARTZMAN

A THESIS SUBMITTED IN PARTIAL FULFILLMENT OF THE

REQUIREMENTS FOR THE DEGREE OF

MASTER OF SCIENCE

IN

OCEANOGRAPHY

UNIVERSITY OF RHODE ISLAND

2018

MASTER OF SCIENCE THESIS

OF

SAMUEL GARTZMAN

APPROVED:

Thesis Committee:

Major Professor Brice Loose

Jaime Palter

James Smith

Nasser H. Zawia
DEAN OF THE GRADUATE SCHOOL

UNIVERSITY OF RHODE ISLAND
2018

ABSTRACT

The Underwater Mass Spectrometer (UMS) provides unprecedented resolution and measurement detail for volatile compounds, including dissolved gases. However, interpretation of the measurements requires attention to several instrumental and environmental effects. We have developed a new calibration method to measure and correct for the influence of hydrostatic pressure, instrument internal temperature, electronic noise, sample temperature, water vapor, and external water temperature changes. We use an in-situ calibration method that samples continuously from a dissolved gas standard; the UMS and in-situ calibration were twice deployed on a submersible tow vehicle to capture profiles throughout the euphotic zone. The primary atmospheric gases - N_2, O_2, Ar and CO_2 - were measured while sampling from the calibration system to examine how independent variables (pressure, internal temperature, electronic noise baseline, sample temperature, water vapor pressure, and in-situ water temperature) cause variability in the UMS readings. Principal Component Analysis was used to evaluate sources of variability and generalized additive models were used to correct the UMS output. These models successfully correct UMS readings to calibrate for ambient sampling within 1% error. In-situ calibration allows for continuous, high fidelity measurements and better tracing of dissolved gases in the ocean.

ACKNOWLEDGMENTS

This thesis would not have been possible without the extreme dedication and support of many people. I am in debt to Dr. Brice Loose for his patience, guidance, knowledge and support as an advisor throughout the process. He pushed me to bring my writing and research to the next level and this work wouldn't be what it is without his help. I would like to thank the support of Dr. R. Timothy Short and Dr. Strawn Toler for their support with method development and data collection. I want to express my gratitude to the science party and crew of cruises EN575 and EN602 onboard the *R/V Endeavor* for their assistance with data collection. I would also like to acknowledge my committee, Dr. Jaime Palter and Dr. James Smith, for their help and guidance on this thesis. Finally, I would like to thank my fellow lab members for their continued encouragement of this work.

TABLE OF CONTENTS

ABSTRACT ii

ACKNOWLEDGMENTS iii

TABLE OF CONTENTS iv

LIST OF TABLES v

LIST OF FIGURES vi

1. INTRODUCTION 1

2. METHODS 4

2.1 Collection Methods 4
2.2 Identifying Sources of Variability 9
2.3 Generalized Additive Modeling 10

3. RESULTS 13

4. DISCUSSION 23

5. CONCLUSIONS 28

APPENDIX 29

BIBLIOGRAPHY 40

LIST OF TABLES

TABLE PAGE

Table 1. The measured masses collected by the UMS and the analyte examined by each mass. 7

Table A1. The timeline of events for EN575. 29

Table A2. The timeline of events for EN602. 33

LIST OF FIGURES

FIGURE PAGE

Figure 1. The cruise tracks of EN575 (March 2016) and EN602 (July 2017). Both cruises followed similar tracks except EN602 left from Gulfport, MS with EN575 leaving from Ft. Lauderdale, FL. 4

Figure 2. The Triaxus tow sled with UMS mounted between the two bottom pontoons. Gas standard box is attached next to the UMS (bottom left). 5

Figure 3. The tow scheme for the Triaxus tow sled with the UMS attached. Black lines are the fiber optic tow cable and red lines are the tow path through the photic zone. .. 6

Figure 4. The membrane inlet assembly that is used on the UMS. The sample is heated to a constant temperature and then pumped into the membrane where it degases into the analysis chamber. The PDMS membrane (inset) is experiencing cyclical compression and decompression during sampling..... 7

Figure 5. The schematic of the inlet tubing for the UMS. The switching valve can be activated from the ship to switch the inlet from the gas-sampling bag or the ambient seawater. During EN575 the switching valve malfunctioned and was removed. The gas-sampling bag was connected directly to the UMS. 8

Figure 6. The conditions during the northward transect of EN575 (left) and EN602 (right). Air temperature, wind speed, mixed layer depth and 1% light level depth trends are depicted. 13

Figure 7. The time series of ion current for each dissolved gas in the gas standard. The top set is from EN575 and the bottom from EN602. 14

FIGURE PAGE

Figure 8. (A) The factor loadings for the first four principal components in the PCA. Factor loadings that are outside of the red lines (>0.5 or <-0.5) constitute large loading on to that component. (B) A biplot showing the groupings of external variables plotted using the loadings of the first two principal components. 15

Figure 9. The time series of the ion current for each dissolved gas (blue) plotted with the pressure reading of the Triaxus (red). The top set is from EN575 and the bottom set is from EN602. 17

Figure 10. Figure 10. The offset (in seconds) of the ion current from the pressure at each direction change of the Triaxus. Every downcast is even and each upcast is odd. Each dissolved gas is represented in a different color. The top panel is from EN575 and the bottom panel is from EN602. 18

Figure 11. The time series of the raw ion current (blue line) and the corrected fit (orange line top row) produced by the GAM for each dissolved gas. The open circles represent the training data that were used to create the GAM parameters. The orange line in the bottom row is the percent error for the corrected fit from the raw ion current. The top set of panels (A) is from EN575 and the bottom set of panels (B) is from EN602..... 19

Figure 12. The ΔAIC_i values for successive additions of input variables into the GAM. Each addition includes the variables previously in the GAM. In every case the GAM with all 6 input variables produced the best fit ($\Delta AIC_i = 0$). The top row is from EN575 and the bottom row is from EN602. 20

FIGURE PAGE

Figure 13. The time series of the raw ion current (blue) during an EN602 bag tow, and corrected fit (orange line top row) using the GAM parameters from a different bag tow. The associated error of this corrected fit is in orange on the bottom row..... 22

Figure 14. The time series of each in-situ calibration on EN602 corrected using the GAM method and converted to O_2 concentration (in μmol/kg) using equation 5. The expected dissolved oxygen content for the 7/13/2017 tow is 215.33 μmol/kg; for the 7/15/2017 & 7/16/2017 tows the expected concentration is 208.11 μmol/kg. 25

Figure A1. The serial cross correlation (red line), plotted in time with the hydrostatic pressure (blue line) during a calibration tow on EN575. 38

Figure A2. The serial cross correlation (red line), plotted in time with the hydrostatic pressure (blue line) during a calibration tow on EN602. 38

Figure A3. Figure A3. The northward transect of dissolved oxygen concentrations measured from the Seabird 43 attached to the Triaxus on EN602. Sampling at the surface of the ocean would not capture the structure seen through the mixed layer depth (red line) and photic zone (purple line). The large amount of oxygen structure in the top 150 meters highlights the potential of UMS measurements to resolve upper ocean structure for many dissolved gases. 39

1. INTRODUCTION

Atmospheric concentrations of greenhouse gases are continually on the rise (Miles, 2009). These changes extend to the ocean as the ocean tends towards equilibrium with the atmosphere. Changes in dissolved gases in the ocean can impact marine life including changes in dissolved minerals necessary for growth (Moore et al., 2013). Dissolved oxygen, which is essential for marine aerobes, is predicted to decline in the oceans over the next century (Keeling et al., 2009). Increased atmospheric warming warms the upper ocean and decreases the solubility of essential dissolved gases, such as nitrogen and oxygen, in seawater. This increased warming also slows ocean mixing and is predicted to decrease the upwelling of nutrients from the deep ocean (Hoegh-Guldberg & Bruno, 2010). While there are many measuring techniques that can determine ocean dissolved gas concentrations, there is a lack of a reliable and accurate in-situ measurement technique that can measure a number of gas concentrations simultaneously (Short et al., 1999).

In the past few decades membrane-inlet mass spectrometry (MIMS) has become a widely used technique and these instruments are getting smaller and more portable (Brennwald et al., 2016; Ferrón et al., 2016; Janfelt et al., 2007; Sommer et al., 2015). MIMS has been used for dissolved gas sensing in a number of applications and is capable of producing comprehensive gas concentration analyses. MIMS incorporates a thin membrane that serves as an interface between the sample and the measurement chamber (Short et al., 1999). This pressure difference between each side of the membrane allows the sample to de-gas into the measurement chamber for analysis

using standard mass spectrometry ionization and detection. MIMS allows continuous measurements of ion currents (relative to the amount of each ion present) to be taken in-situ for up to 12-hour segments at a time (Short et al., 1999; Sysoev, 2000).

Recently MIMS has been used for detecting dissolved gas concentrations – generally through a ship's flow through system – to get in-situ surface gas concentrations (Ferrón et al., 2016). However, only a few groups have been able to design and implement MIMS measurements at different depths (Bell et al., 2007, 2012; McMurtry et al., 2012). Bell et al. (2007) used specialized instrumentation that allowed the first in-situ measurements of real time vertical profiles of gas concentrations in the ocean. However, putting a MIMS to depth comes with a number of challenges— the largest of which is accounting for the signal drift due to hydrostatic pressure changes through the water column (Bell et al., 2007). While semi empirical calibrations have been made (Bell et al. 2007) we describe a way to obtain a more robust calibration. We place a gas-sampling bag filled with a constant concentration of dissolved gasses with the Underwater Mass Spectrometer (UMS) to expose the bag to the ambient pressure that the UMS experiences through the upper ocean. We find the in-situ calibration to be a better method to represent the depth changes, which leads to a better calibration of the UMS. This can also allow for the instrument to stay at depth for longer and calibrate with just a switch to the standard bag for a few cycles. With the expectation that the concentration from the bag should read a constant value, the data collected from the in-situ bag tows can be used to model the effects of external variables (such as hydrostatic pressure) on the UMS. The

modeled effects could then be used to remove the external effects from the marine dissolved gas signal.

In this study, we use in-situ gas-sampling bags to aid in modeling changes through the water column to ensure an improved calibration of the UMS. We hope to answer the following questions: 1) What variable(s), in addition to hydrostatic pressure, cause variability in the UMS output during depth changes? 2) How can we best account for this variability to improve in-situ data from the UMS?

2. METHODS

2.1 Collection Methods

Underwater mass spectrometry measurements were taken aboard the *R/V Endeavor* during cruises EN575 and EN602 in March 2016 and July 2017 respectively. EN575 traveled from Ft. Lauderdale, FL to Narragansett, RI and EN602 departed Gulfport, MS through the Gulf of Mexico and northward to Narragansett, RI. Cruise tracks were designed to enter into the Atlantic subtropical gyre and cross the Gulf Stream (Figure 1). The EN602 cruise track was modeled to match the previous cruise track after sailing north of Ft. Lauderdale, which allowed for repeated sampling in different seasonal conditions.

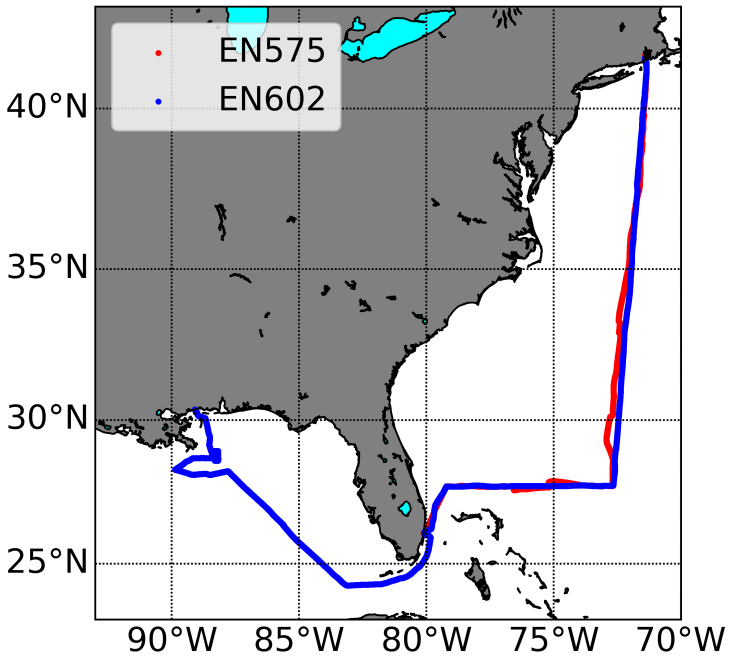

Figure 1. The cruise tracks of EN575 (March 2016) and EN602 (July 2017). Both cruises followed similar tracks except EN602 left from Gulfport, MS with EN575 leaving from Ft. Lauderdale, FL.

The UMS, manufactured by SRI International, was attached to a Triaxus tow sled (Figure 2). The Triaxus tow sled was set to follow tow-yo operations (Figure 3) between 5-200 meters over while sampling from gas-sampling bags. A tow-yo consists of the Triaxus undulating between the surface and a specified depth while being towed by the ship. The ship speed ranged from 7 to 10 knots while the Triaxus

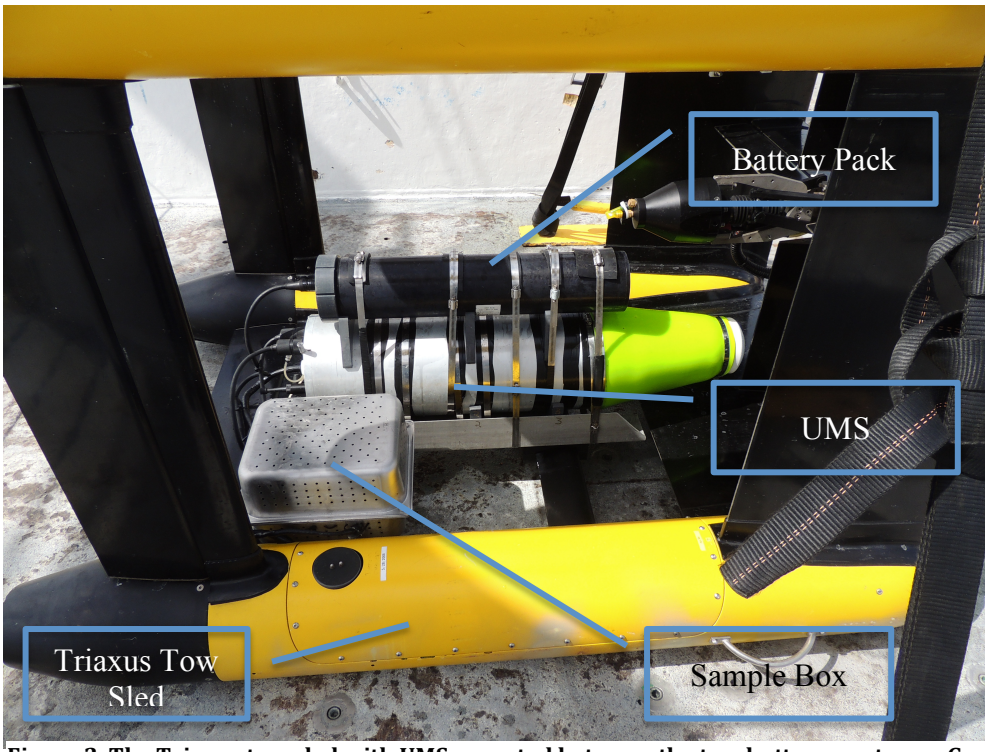

Figure 2. The Triaxus tow sled with UMS mounted between the two bottom pontoons. Gas standard box is attached next to the UMS (bottom left).

would travel through the water column. The UMS monitored the masses listed in Table 1 simultaneously with a 256 ms dwell time, the duration in which each molecular mass ion signal is collected. Each measured mass is measured as ion current, which is porportional to the relative concentrations of each dissolved analyte. All data was logged on a laptop merging data streams from the Conductivity,

Temperature and Depth (CTD) sensor, Triaxus, and UMS in real time using a custom Lab View software program (provided by SRI International). There is a length of tubing that seawater is pumped through, which delays the UMS reading compared to

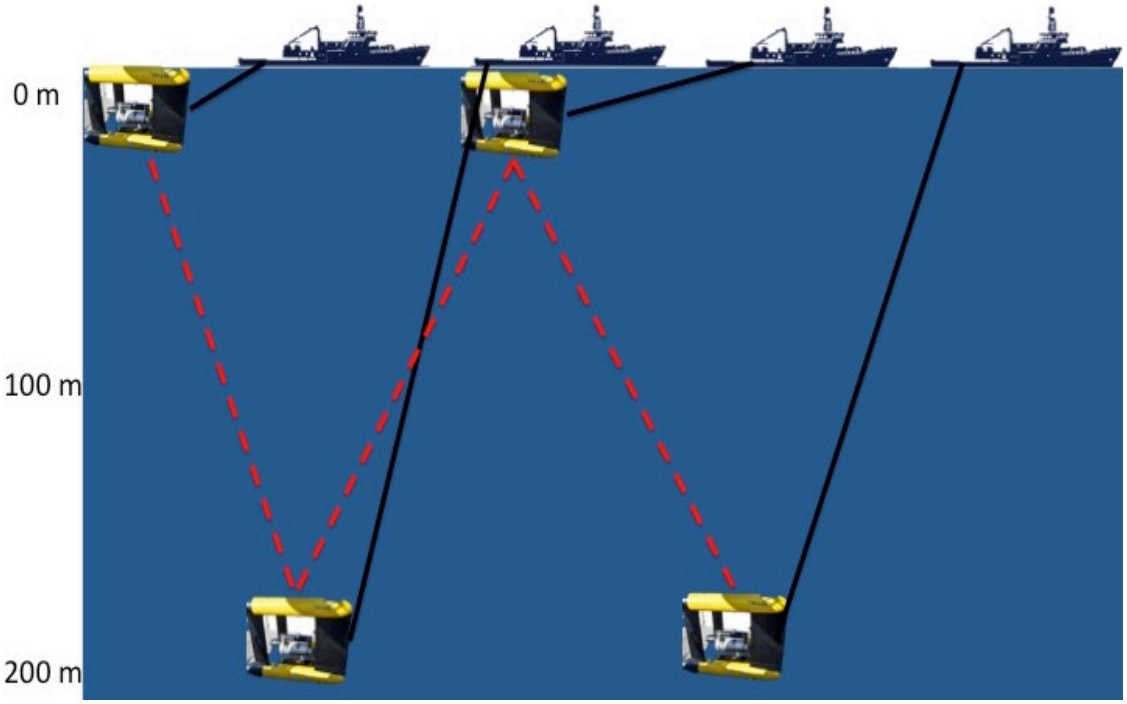

Figure 3. The tow scheme for the Triaxus tow sled with the UMS attached. Black lines are the fiber optic tow cable and red lines are the tow path through the photic zone.

the CTD data. In order to account for this lag, we measured the delay at multiple times throughout each cruise. Before any data analysis, the UMS data was shifted in time to match up with the CTD data stream. Mixed layer depth was calculated from the CTD pressure and temperature data. The mixed layer was determined by searching for the first occurrence of a change in potential density greater than 0.05 kg/m^3 above the surface reference density value (Brainerd & Gregg, 1995). The UMS has a Polydimethylsiloxane (PDMS) membrane assembly, which is depicted in Figure 4. Sample flow into the membrane assembly was 14 mL/min with a membrane temperature of 35˚C.

Table 1. The measured masses collected by the UMS and the analyte examined by each mass.

Mass (*mass/charge*)	**Factor**	**Mass** (*mass/charge*)	**Analyte**
5	Electronic Baseline	28	Nitrogen (N_2^+)
18	Water Vapor (H_2O^+)	32	Oxygen (O_2^+)
		40	Argon (Ar^+)
		44	Carbon Dioxide (CO_2^+)

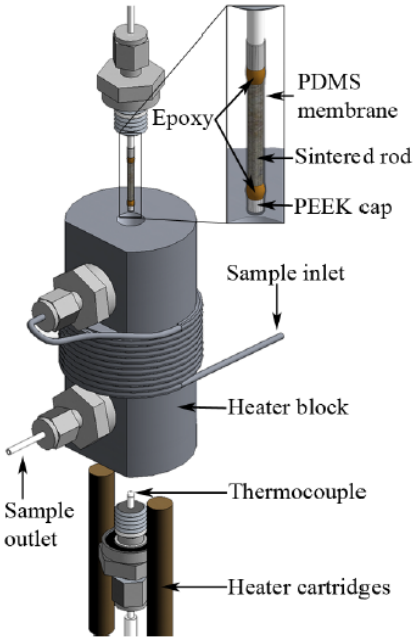

Figure 4. The membrane inlet assembly that is used on the UMS. The sample is heated to a constant temperature and then pumped into the membrane where it degases into the analysis chamber. The PDMS membrane (inset) is experiencing cyclical compression and decompression during sampling. Image from (Bell et al., 2007).

A small, sample box with perforated edges was also attached to the tow sled, which contained a 1 L or 2 L gas tight sampling bag (Figure 1). The perforations allowed seawater to floe through the box so that each bag would experience ambient hydrostatic pressure and temperature inside the container. Each bag contained seawater that was equilibrated with a mixture of gas standards. For EN575 the gas mixture was 0.100% CH_4, 0.600% Ar, 23.000% O_2, and Balance N_2. During EN602

the mixture contained 0.100% CH_4, 1.000% Ar, 20.900% O_2, and Balance N_2.The gas standards were bubbled in seawater with a 0.02 µm pore frit for at least twenty minutes and then transferred to the gas tight sampling bag via peristaltic pump to ensure equilibrium with the gas standard and no introduction of atmospheric air bubbles. The initial setup of the gas-sampling bag consisted of a connection to the UMS via a solenoid switching valve allowing the ability to switch between ambient seawater and standard equilibrated seawater (Figure 5). This valve malfunctioned midway through EN575, requiring the bags be connected directly to the UMS for all bag tows from then on. During EN602 the switching valve was replaced and activated remotely for in-situ calibration from the ship.

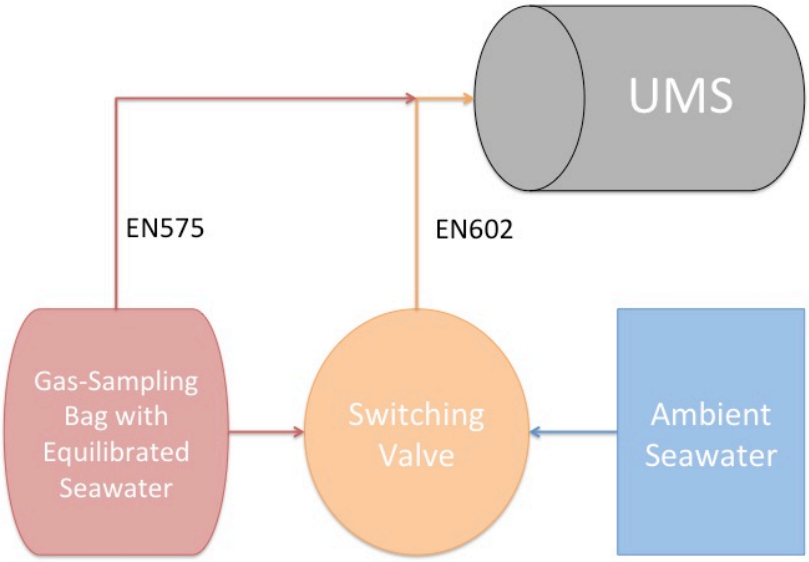

Figure 5. The schematic of the inlet tubing for the UMS. The switching valve can be activated from the ship to switch the inlet from the gas-sampling bag or the ambient seawater. During EN575 the switching valve malfunctioned and was removed. The gas-sampling bag was connected directly to the UMS.

2.2 Identifying Sources of Variability

The ion currents corresponding to each mass/charge (m/z) ratio listed in Table 1 were plotted with depth to visualize the anticipated pattern corresponding with pressure changes throughout the tow-yo. To search for any offset in the UMS response to pressure changes, a serial cross correlation was used to calculate lag between ion current and pressure. Serial cross correlation examines the correlation of two time series at different temporal displacements (Rabiner & Gold, 1975). In our application, the convolution of the ion current and pressure are integrated at every time lag to reach a correlation value (Rabiner & Gold, 1975). In addition, we used principal component analysis (PCA), combined with calculated factor loadings, to identify where the ion current variability is derived. PCA is a multivariate statistical method that transforms the original variables into linear combinations (principal components) that account for most of the variation in the original variables (James et al., 2013). In PCA an $n \times m$ matrix is created, $\boldsymbol{X}$, where there are n observations with m variables. Using singular value decomposition we can derive equation 1 (Glover et al., 2011):

$$\boldsymbol{X} = \boldsymbol{USV'} \tag{1}$$

where $\boldsymbol{U}$ is an orthonormal matrix containing n eigenvectors of the major product of $\boldsymbol{X}$, $\boldsymbol{V}$ is an orthonormal matrix containing m eigenvectors of the covariance matrix of $\boldsymbol{X}$, and $\boldsymbol{S}$ is a square matrix with diagonal elements of the non-negative singular values of $\boldsymbol{X}$ (Glover et al., 2011). The matrix, $\boldsymbol{V}$, is made with vectors that are uncorrelated, but account for the maximum variance in $\boldsymbol{X}$. The components are ordered in the amount of variance they account for, the first containing the most variance and the second with

the next most (James et al., 2013). The covariance matrix of $\boldsymbol{X}$, $\boldsymbol{R}$, is then used in equation 2:

$$\boldsymbol{RV} = \boldsymbol{V\Lambda} \tag{2}$$

with $\boldsymbol{V}$ containing the eigenvectors of $\boldsymbol{R}$ and $\boldsymbol{\Lambda}$ containing the eigenvalues ($\boldsymbol{\lambda}$) on its diagonal (Glover et al., 2011). To examine the relative contribution of each original variable to the newly calculated principal components (with vectors $\boldsymbol{V}$ and values $\boldsymbol{\lambda}$), we can calculate the factor loadings. Factor loadings, $\boldsymbol{A}$, are computed through equation 3:

$$\boldsymbol{A} = \boldsymbol{VS} = \boldsymbol{V}\sqrt{\boldsymbol{\Lambda}} \tag{3}$$

These factor loadings are the building blocks of the principal components and tell you the relative contribution of each input variable to the principal components. For our PCA, we used mass 5, 28, 32 40 and 44 ion currents, pressure, internal temperature, and time as the input variables ($\boldsymbol{X}$). Comparison of each principal component for the ion currents with the supposed "independent" variables, such as hydrostatic pressure, provide an indication of which terms are correlated, not-correlated or anti-correlated, and the relative dominance of each correlation. We used the factor loadings to help us understand the external variables that were producing the most variance in the UMS output. These sources of variability helped guide the corrections that were needed for the in-situ measurements of the UMS.

2.3 Generalized Additive Modeling

Generalized additive modeling is a way to predict a dependent variable by individually fitting to a set of independent variables. A generalized additive model (GAM) is created by taking individual, non-linear fits between each independent variable and the

dependent variable (James et al., 2013). These non-linear fits are then added together as described in equation 4:

$$\boldsymbol{Z = b_0 + f_1 * X_1 + \cdots + f_m * X_m} \quad (4)$$

where $\boldsymbol{Z}$ is the predicted values of the dependent variable, where $\boldsymbol{X_1}$ through $\boldsymbol{X_m}$ are the values of the predictor variables, $\boldsymbol{b_0}$ is a coefficient determined by semi-parametric multivariate regression, and $\boldsymbol{f_1}$,through $\boldsymbol{f_m}$ are the functions determined by using penalized splines that keep the additive nature of each predictor variable (Hill & Lewicki, 2006). GAMs are useful to fit a non-linear function to each $\boldsymbol{X_m}$, while the the model can also show the individual effect each $\boldsymbol{X_m}$ can have on $\boldsymbol{Z}$ (James et al., 2013).

In our application of GAM, we used water vapor (taken as mass 18), pressure, sample temperature, internal temperature, water temperature and electronic noise (taken as mass 5) as predictor variables. A different GAM was produced for each dissolved gas of interest in the seawater standard (Nitrogen, Oxygen, Argon and Carbon dioxide). The pyGAM toolbox was used to create the GAM in python programming language (Servén, January 19, 2017/2018). A random sample of 10% of the bag tow was used to train the GAM. The complementary 90% of the bag tow data was used to evaluate the fit of each GAM.

The ion current for each dissolved gas of interest was divided by its corresponding GAM to reach a predicted fit. A linear, two point calibration was performed by using equation 5:

$$\boldsymbol{F} = \frac{[\boldsymbol{C}]}{(\boldsymbol{I_n} - \boldsymbol{I_0})} \quad (5)$$

where $\boldsymbol{F}$ is the calibration factor, $\boldsymbol{[C]}$ is the concentration of the gas in the bag (determined by gas solubility), $\boldsymbol{I_n}$ is the average predicted ion current in the bag, and $\boldsymbol{I_0}$ is the ion current when water has completely degassed into the membrane of the UMS and all of the dissolved gas has been depleted out of the sample. This calibration factor was multiplied by the test set of ion current data to reach a calibrated concentration in μmol of gas per kg of seawater.

3. RESULTS

Along the northward transect of EN575 there was a mean air temperature of 18.11˚ ± 1.93˚C with a mean wind speed of 14.33 ± 7.56 knots. The high wind speeds in conjunction with the colder air temperatures provided the conditions for deeper mixed layers. In contrast, EN602 had a mean air temperature of 26.63˚ ± 3.12˚C and mean wind speeds of 9.72 ± 4.18 knots (Figure 6). These lower wind speeds and higher temperature produced the conditions for increased stratification in the upper ocean. Stratification occurs when there is little wind driven mixing and an increased short wave radiation flux into the ocean (Talley, 2011).

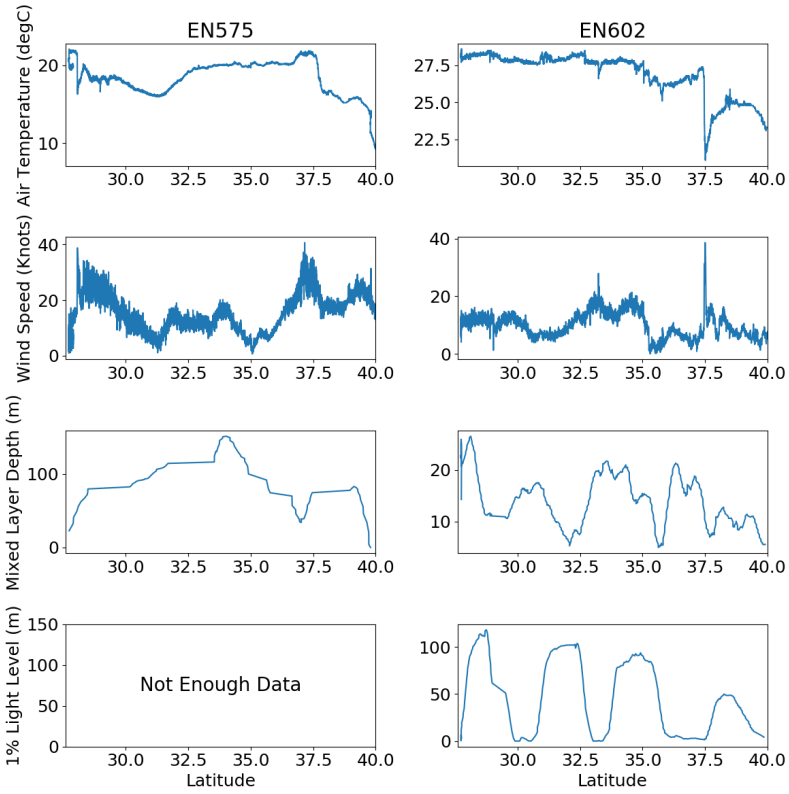

Figure 6. The conditions during the northward transect of EN575 (left) and EN602 (right). Air temperature, wind speed, mixed layer depth and 1% light level depth trends are depicted.

During the bag calibrations successive dives of the Triaxus the ion currents of each dissolved gas decreased with increased depth. This parabolic time series, at first, suggests a strong pressure dependence on the dissolved gas readings (Figure 7).

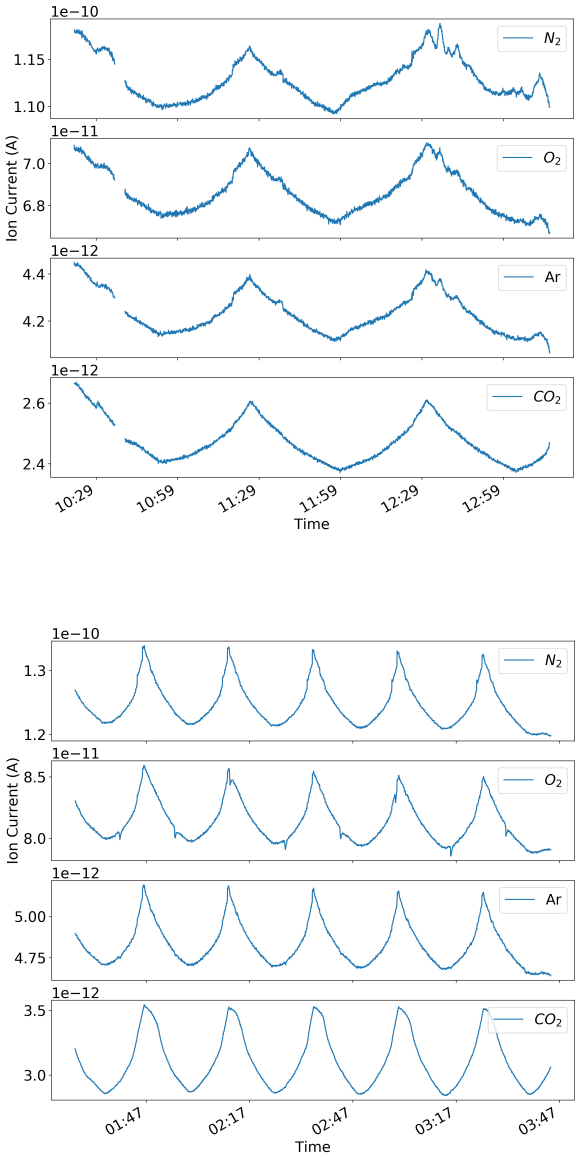

Figure 7. The time series of ion current for each dissolved gas in the gas standard. The top set is from EN575 and the bottom from EN602.

This pressure dependence has been previously studied in Bell et al. 2012, but our PCA results have been able to suggest other external variables that cause variability in the readings of the UMS.

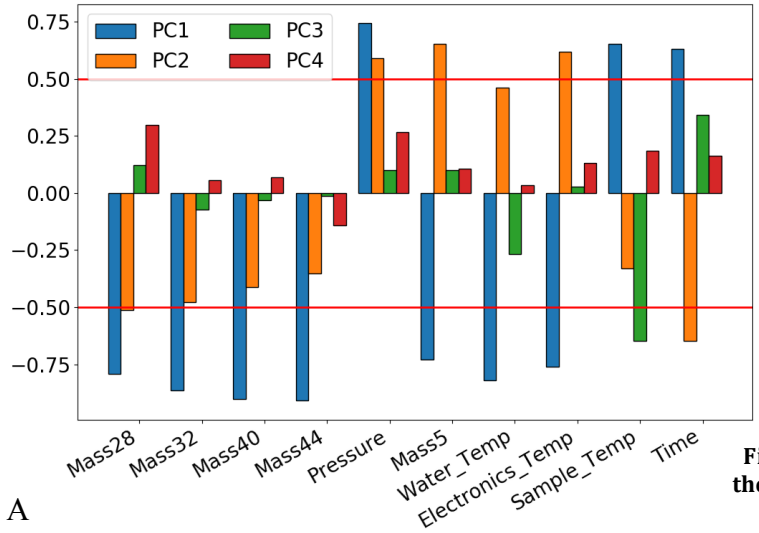

A

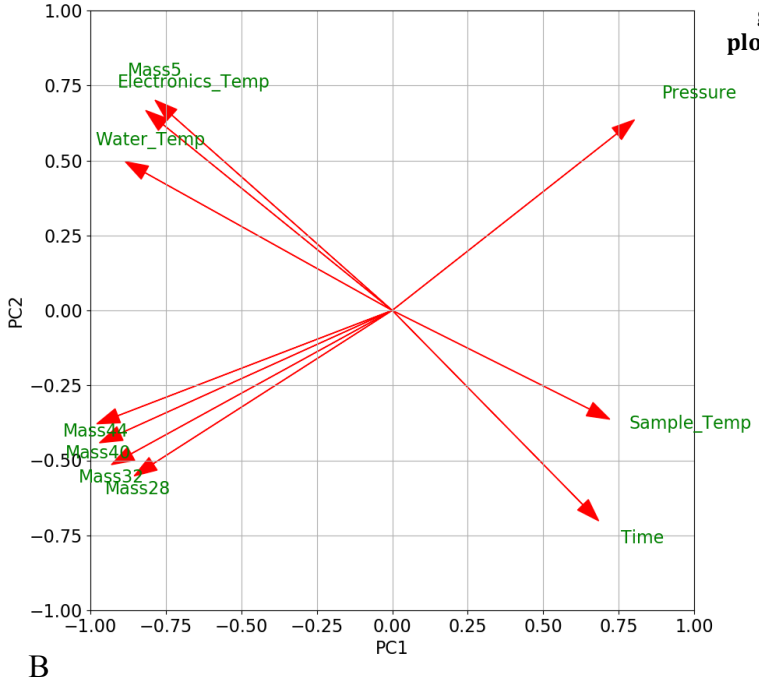

B

Figure 8. (A) The factor loadings for the first four principal components in the PCA. Factor loadings that are outside of the red lines (>0.5 or <-0.5) constitute large loading on to that component. (B) A biplot showing the groupings of external variables plotted using the loadings of the first two principal components.

The factor loading analysis (Figure 8a) shows where the principal components correlate with independent environmental variables. Large (over 0.5 or less than -0.5) loadings of pressure, electronic noise, water temperature, electronics temperature, sample temperature and time are observed. These large loadings allow us to infer that these independent variables can be causing the variability associated with that principal component (Jolliffe, 1986). The biplot (Figure 8b) allows interpretation of the two principal components containing the largest variability in the input data and the relationship of the input data to those variables. Variables that are grouped together have a similar effect on the variability (Jolliffe, 1986). Due to the large loadings and the relatively large number of groupings in the biplot, we concluded that there are a number of different processes affecting the UMS output. We decided to include all of the independent input variables into the correction process as a way that would best model the UMS variability.

To get a better understanding of the effect of time and lag on the variability, a serial cross correlation was completed. The serial cross correlation alerted us to an offset between the local extrema of the pressure vector and the local extrema of the ion current. In Figure 9 it is fairly clear that these two time series are slightly offset. To get a better understanding how this offset changed over time, we plotted the offset between the ion current and the pressure vector for each time the Triaxus changed direction. Figure 10 shows this intriguing trend where there seems to be an alternating pattern of the pressure leading the ion current and then lagging behind (or closely leading) the ion current. The response of the membrane was slightly different between

EN575 and EN602. We attribute these differences to the fact that during EN602 the UMS was able to stay in the water much longer with the functioning switching valve. PDMS membranes behave differently with repeated compression (Futó & Degn, 1994). The small differences in offset between the cruises are likely due to different membrane behavior (*See Discussion*).

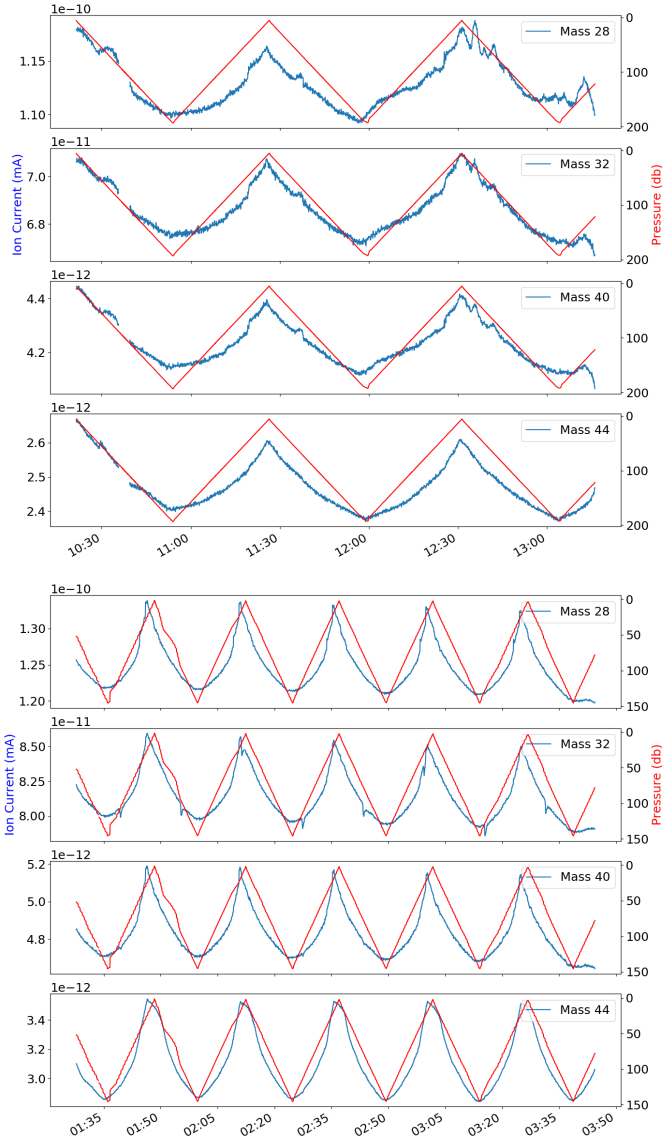

Figure 9. The time series of the ion current for each dissolved gas (blue) plotted with the pressure reading of the Triaxus (red). The top set is from EN575 and the bottom set is from EN602.

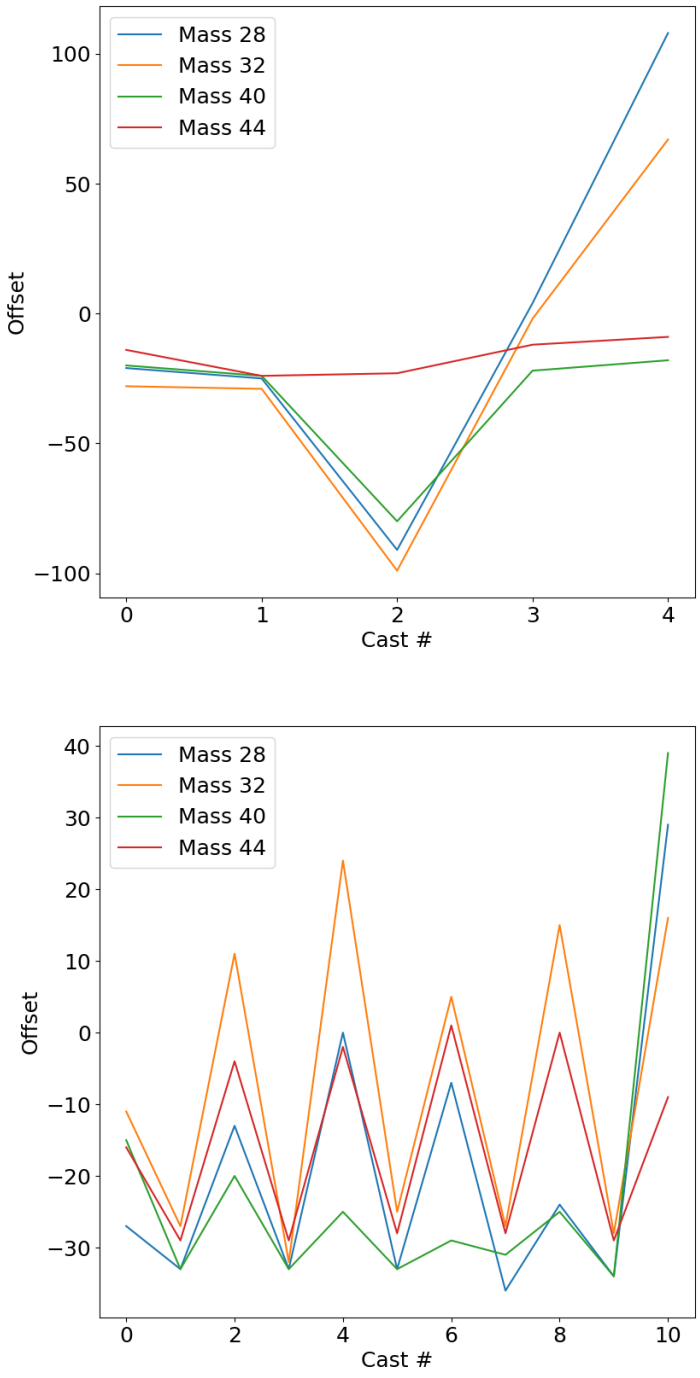

Figure 10. The offset (in seconds) of the ion current from the pressure at each direction change of the Triaxus. Every downcast is even and each upcast is odd. Each dissolved gas is represented in a different color. The top panel is from EN575 and the bottom panel is from EN602.

Figure 11 shows the implementation of the GAM to the in-situ bag calibration data. The open circles show the training data and the orange line is the predicted ion current from the GAM of each dissolved gas. Only with 10% of the data used for training

normalized residuals show a mean of 0.27% error (± 0.051%). The GAM is able to empirically model the behavior of the UMS.

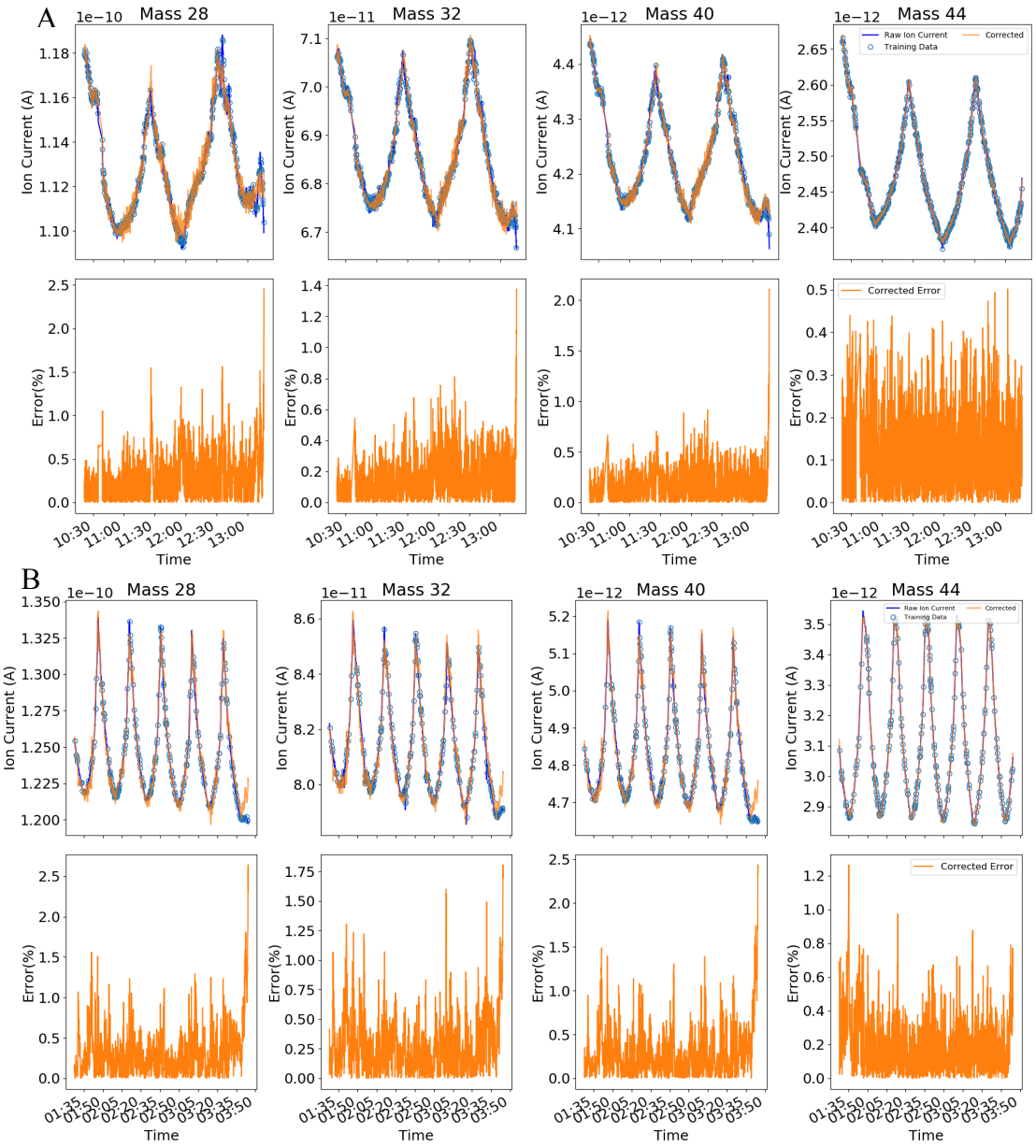

Figure 11. The time series of the raw ion current (blue line) and the corrected fit (orange line top row) produced by the GAM for each dissolved gas. The open circles represent the training data that were used to create the GAM parameters. The orange line in the bottom row is the percent error for the corrected fit from the raw ion current. The top set of panels (A) is from EN575 and the bottom set of panels (B) is from EN602.

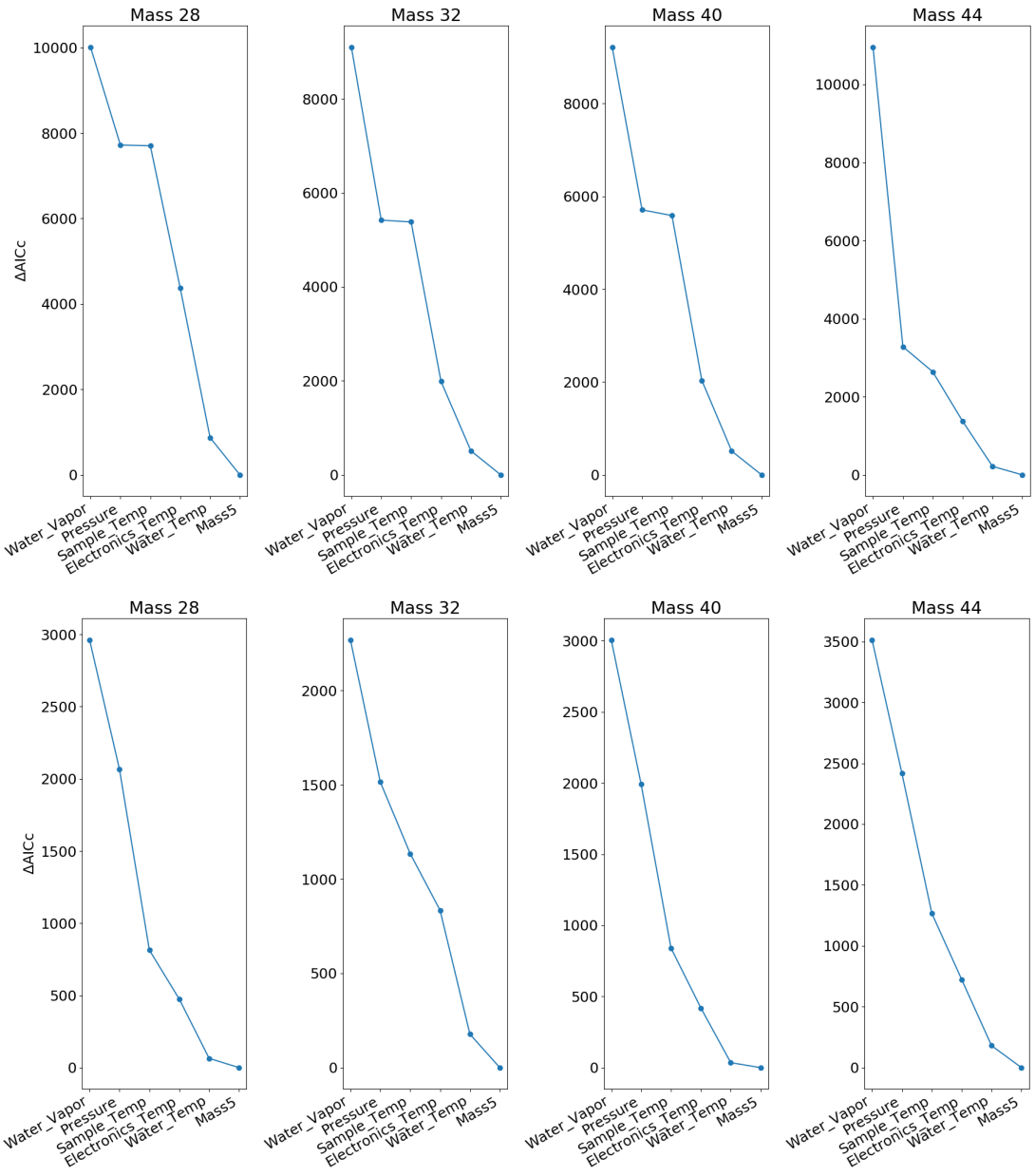

Figure 12. The ΔAIC_i values for successive additions of input variables into the GAM. Each addition includes the variables previously in the GAM. In every case the GAM with all 6 input variables produced the best fit ($\Delta AIC_i = 0$). The top row is from EN575 and the bottom row is from EN602.

The Alkaike information criterion (AIC) is an estimator of the quality of fit of a statistical model (Akaike, 1974). When a number of models are fit to the same data, AIC can be used to ensure the best relative quality to each other and can help chose the best model (Burnham & Anderson, 2004). AIC is based upon maximizing the log likelihood function, $\hat{\boldsymbol{L}}$, for the model. The maximum is placed into equation 6:

$$\boldsymbol{AIC = 2k - 2ln(\hat{L})} \quad (6)$$

where, $\boldsymbol{k}$, is the number of estimated parameters (Burnham & Anderson, 2004). However, AIC doesn't prove to be a good estimator when the sample size is small. This bias, however, is corrected for in the AIC_c equation:

$$\boldsymbol{AIC_c = 2k - 2ln(\hat{L}) + \frac{2k^2 + k}{n - k - 1}} \quad (7)$$

where $\boldsymbol{n}$ is the sample size. AIC_c converges to AIC when the sample size is large and thus is better to use for our application (Burnham & Anderson, 2004). The individual AIC (or AIC_c) values don't have meaning unless they are rescaled to its relative values:

$$\boldsymbol{\Delta AIC_i = AIC_i - AIC_{min}} \quad (7)$$

These relative values can show how each GAM fits to the target data normalized to the GAM with the lowest AIC, which is the best fitting model to the target data. GAMs having $\boldsymbol{\Delta AIC_i} \leq 2$ have substantial support (evidence), those in which $4 \leq \boldsymbol{\Delta AIC_i} \leq 7$ have considerably less support, and GAMs having $\boldsymbol{\Delta AIC_i} > 10$ have essentially no support that they fit the data better than the GAM with the minimum AIC value (Burnham & Anderson, 2004; Stone, 1977). In an effort to test the relative effects of each of our input variables, unique GAMs were made in succession adding one variable at a time to the fitting parameters. $\boldsymbol{\Delta AIC_i}$ was calculated for each model (Figure 12). For each dissolved gas the model with all 6 parameters shows the lowest $\boldsymbol{\Delta AIC_i}$ (equaling 0). All other $\boldsymbol{\Delta AIC_i}$ values not close (>10) to each other, which suggest that the less sophisticated models show little support of modeling the fit better than model with all input factors. Through the AIC analysis, we concluded that over fitting was not occurring in our GAM because the full GAM had the lowest AIC.

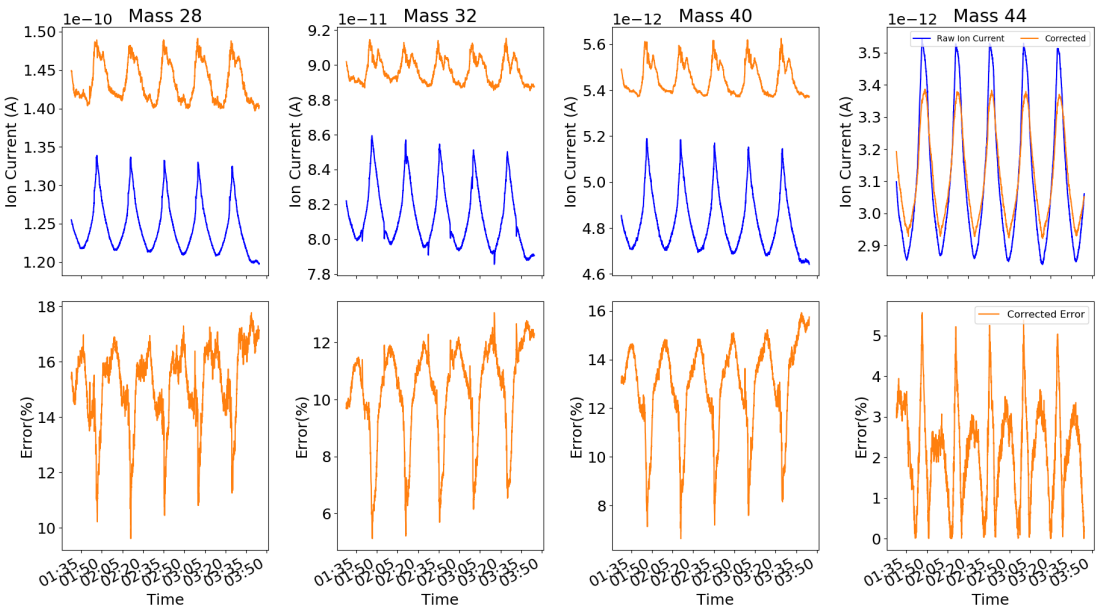

Figure 13. The time series of the raw ion current (blue) during an EN602 bag tow, and corrected fit (orange line top row) using the GAM parameters from a different bag tow. The associated error of this corrected fit is in orange on the bottom row.

In an effort to test the universality of this new calibration method, the GAM parameters created for one calibration were applied to another calibration tow. Figure 13 shows the relatively large errors that are created with these corrections. Every time we take the UMS out of the water and power the system back up seems to change the response of the system. While this study has not been able to find what could be causing this shift in readings, it reinforces the fact that the UMS should be calibrated regularly to account for any drift or shift in UMS output. Even with drifts that occur in the instrument, regular calibrations with our GAM methods would be able to refit according to the shifts that may occur.

4. DISCUSSION

The results presented here demonstrate that our calibration methods are able to successfully capture the environmental variability for ocean applications. The PCA has instructed our method in finding the independent variables that are causing variability in the bag tows. We have been able to independently account for each of these variables through GAMs. These models are able to capture the variability at all depths and provide a generalized way to reproduce the effect of each predictor variable.

In an effort to ensure the best possible predictor method for the UMS, we went through a number of iterations for the calibration before settling on the GAM method presented. We started to use successive polynomial fits to try to capture the external variables. These polynomial fits were originally trained with the first downcast and tested on the rest of the bag tow. While downcasts were well modeled, we observed degradation of the fit in each of the upcast. These fits also were not satisfactorily made to capture the transition zones from downcast to upcast or upcast to downcast. In the next iteration we differentiated the downcast and upcast by training each one individually on the first cycle and testing the respective fits to the rest of the cast. In this iteration we were able to capture the differences in upcast and downcast, but still weren't able to model the transition zones. The GAM method provided us a way to capture the additive nature of successive fits, by fitting each parameter simultaneously. This simultaneous fitting has proven to capture the transition zones and minimize the modeled error in both upcasts and downcasts. In the GAM method we also moved to

training on a random sampling of 10% of the data. The current train/ test split gave the model added predictive power to longer-term changes that the UMS experiences throughout the whole bag tow. We find the GAM method to be generalized, but also provides a high quality fit.

During each in-situ calibration on EN602 we have been successful at removing the variation from external variables and just measuring the bag concentration, which is constant for the entire tow. Figure 14 shows this high quality fit for dissolved oxygen (mass 32) throughout EN602 after conversion to concentration units. For the 7/13/2017 in-situ calibration the dissolved oxygen content (based on solubility) is 215.33 μmol/kg; for the 7/15/2017 and 7/16/2017 in-situ calibrations the dissolved oxygen content is 208.11 μmol/kg. The constant and accurate values of the calibrated UMS readings proves that this calibration is successful in converting UMS ion current to concentrations without the effects of external variability.

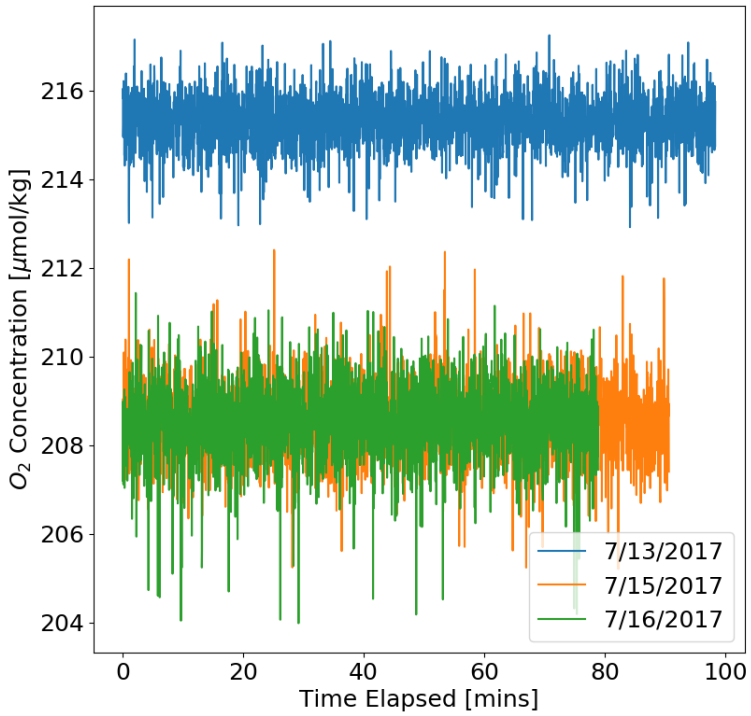

Figure 14. The time series of each in-situ calibration on EN602 corrected using the GAM method and converted to O_2 concentration (in µmol/kg) using equation 5. The expected dissolved oxygen content for the 7/13/2017 tow is 215.33 µmol/kg; for the 7/15/2017 & 7/16/2017 tows the expected concentration is 208.11 µmol/kg.

One challenge with membrane inlet systems is the nature of PDMS compression and decompression. The typical response for cyclic compression in PDMS is hysteresis. The unloading path is composed of less stress than the loading path. Previous studies attribute this hysteresis effect to the non-linear elastic deformation of the membrane (Futó & Degn, 1994; Lee et al., 2016). In addition to the hysteresis of PDMS, after continued cyclic compression of PDMS a process called strain hardening occurs. In this process the membrane strengthens to with repeated compression. The hardening of the PDMS has been studied to level off after a number of cycles, but results have shown that hardening could occur past 100 cycles (Lee et al., 2016). The PDMS

hardening over multiple cycles supports the choice to use training data over the whole calibration instead of the first cycle. We have seen this hardening and non-linear response in the serial cross-correlation and the lag between the ion current and pressure. Even with the lag response in the system, we have been able to fit accounting for this lag response in the GAM.

We attributed the differences in offset between EN575 and EN602 to the lag effect. Since we had the ability to switch to the bag remotely during EN602, we were able to have the Triaxus in the water for longer transects compared to EN575. We suspect these longer transects shifted the PDMS membrane to the more hardened state, which could account for the difference in offset seen in Figures 9 and 10 between EN575 and EN602. However, another condition that changed between cruises was the in-situ water temperature. On EN602 the water temperature was generally higher and the heater block (Figure 4) didn't have to work as much at the surface. As a result of the warmer surface water the heating duty cycle relaxed near the surface and cooled the membrane prematurely, which could allow for the peak in ion current before reaching minimum pressure. Likely the membrane behavior in EN602 was influenced both by the heating cycles and the PDMS strain hardening. In the GAM we account for the heating cycle by including the sample temperature, which is why this offset isn't a source of error in the final results.

While we have had a lot of success in capturing the external variability imposed on the UMS, there are still areas to improve. As discussed earlier, the UMS seems to produce

a different output every time it is power cycled and put into the water. While we haven't been able to find the cause of this cruise drift, we can account for this drift by calibrating at various points throughout the cruise. This calibration method could be improved to be able to create a GAM that could be applied to the entire cruise instead of just sections close to where the calibration occurred. In an ideal world, a cruise would only need a few calibrations that would be able to correct all of the data, which would focus in-water time on collecting ambient data.

5. CONCLUSIONS

In this study we have been able to utilize the simultaneous in-situ sampling from underwater mass spectrometer and create a calibration method with average accuracy within 1%. This study has demonstrated that the lag that occurs with UMS sampling can be accounted for using water vapor, pressure, internal temperature, water temperature, electronic noise and sample temperature. The in-situ calibration allows for almost identical conditions to ambient sampling, which previous calibration methods have not been able to accomplish. This calibration method opens the possibility for use in resolving physical processes in both vertical and horizontal scales through the tow-yo technique. In addition, this calibration could also be used on vertical sampling from a rosette frame during CTD casts. The UMS has many possibilities for ocean tracing and sampling such as examining net community production via O_2/Ar ratios, which is an ongoing area of discussion in the oceanographic community (Ducklow & Doney, 2013; Reuer et al., 2007). Dissolved gas concentrations are proxies for tracing to understand mixing and uptake of nutrients. Since gases' diffusion into and through ocean is relatively well studied, the UMS opens the way to look at fine scale gas concentration changes in real time. Atmospheric greenhouse gas concentrations are not predicted to decrease any time soon, and their uptake by the ocean will continue to increase (Miles, 2009). The in-situ calibration allows these increasing greenhouse gas concentrations to be measured more readily and with higher spatial resolution. More quantitative calibration of UMS sampling will help advance the use of UMS as an ocean sampling technique and can help the understanding of dissolved gases in the world's oceans.

APPENDIX

Table A1. The timeline of events for EN575.

Date (GMT)	Time (GMT)	Latitude	Longitude	Triaxus Status	Event	Notes
03/03/16	16:30	26.0898	-80.11564	In Water	Triaxus Deployed for dunk test	UMS coms not functioning
03/03/16	14:58	26.08983	-80.1156	On Deck	Left Ft. Lauderdale, FL	
03/04/16	12:05	27.73131	-76.97905	On Deck	UMS Powered Up- Started Logging	
03/04/16	12:24	27.7324	-76.94485	In Water	Triaxus in Water	
03/04/16	13:50	27.72167	-76.82549	In Water	O2 sensor failed	
03/04/16	16:49	27.71954	-76.39308	In Water	Triaxus lost power	
03/04/16	17:00	27.71838	-76.37297	On Deck	Triaxus Recovered	
03/04/16	17:23	27.70819	-76.36573	On Deck	Stopped Logging	
03/05/16	1:51	27.59032	-76.54983	On Deck	UMS Powered Up- Started Logging	
03/05/16	1:54	27.59036	-76.55142	In Water	Triaxus in Water (5-200 m dives)	
03/05/16	8:30	27.65065	-75.86587	In Water	New file started	
03/05/16	13:18	27.68747	-75.3108	In Water	Switching valve ON	No signal change
03/05/16	14:28	27.69163	-75.17953	In Water	Triaxus Issues - Stopped Logging	
03/05/16	14:35	27.69461	-75.17652	On Deck	Triaxus Recovered	Deck valve test, change O2 sensor
03/05/16	17:56	27.74671	-75.2082	On Deck	UMS Powered Up- Started Logging	
03/05/16	18:05	27.74962	-75.2091	In Water	Triaxus in Water	
03/05/16	18:12	27.7528	-75.20712	In Water	Switching valve ON	Valve failure
03/05/16	18:18	27.75345	-75.19906	On Deck	Triaxus Recovered - UMS humidity high	
03/05/16	18:27	27.75509	-75.19596	On Deck	Stopped Logging	No water in UMS housing
03/05/16	23:33	27.86205	-75.19358	On Deck	UMS Powered Up- Started Logging	

03/05/16	23:38	27.86332	-75.19313	In Water	Triaxus in Water	
03/05/16	23:49	27.86852	-75.18987	In Water	Switching valve ON	Valve failure
03/05/16	23:53	27.8708	-75.18703	In Water	Switching valve ON	Valve failure
03/06/16	0:09	27.8839	-75.16015	In Water	Switching valve ON	Valve failure
03/06/16	0:12	27.88582	-75.15312	In Water	Starting tow yo (5-200 m)	
03/06/16	3:37	27.87225	-74.66329	In Water	New file started	
03/06/16	3:38	27.87201	-74.66092	In Water	Switching valve ON	Valve failure
03/06/16	4:14	27.86006	-74.57643	In Water	Switching valve ON	Valve failure
03/06/16	5:01	27.84841	-74.46629	In Water	New file started	
03/06/16	5:05	27.84758	-74.4568	In Water	Starting tow yo (5-200 m)	
03/06/16	9:42	27.75296	-73.82801	In Water	CTD cut out	
03/06/16	11:31	27.75466	-73.57169	In Water	CTD cut out	
03/06/16	11:58	27.75039	-73.49703	In Water	CTD cut out	
03/06/16	12:41	27.7394	-73.37377	In Water	CTD cut out	O2 data is not coming in as umol/kg
03/06/16	13:52	27.72775	-73.17104	In Water	Shallower dives for CTD cast (5-20 m)	
03/06/16	14:01	27.72622	-73.14555	In Water	New file started	
03/06/16	15:31	27.74036	-73.08207	In Water	Switching valve ON	No tow yos
03/06/16	16:51	27.74027	-72.8897	In Water	Switching valve OFF	No tow yos
03/06/16	16:56	27.73989	-72.87594	In Water	New file started (5-200 m)	
03/06/16	17:40	27.73595	-72.75739	In Water	O2 data as voltage	
03/06/16	23:00	28.45224	-72.68436	In Water	Increased sea state, slowed 5 knots	
03/06/16	23:41	28.50434	-72.68052	On Deck	Triaxus Recovered - Stopped logging	
03/07/16	1:00	28.53344	-72.68027	On Deck	Transiting overnight for better weather	
03/07/16	20:38	30.16101	-72.70168	On Deck	UMS Powered Up- Started Logging	No PAR sensor
03/07/16	20:40	30.16199	-72.70047	In Water	Triaxus in Water	No CTD Data
03/07/16	20:43	30.16346	-72.69856	In Water	CTD On	
03/07/16	20:54	30.17758	-72.69025	In Water	Starting tow yo (5-200 m)	
03/07/16	21:09	30.20531	-72.68513	In Water	Triaxus lost coms	

03/07/16	21:14	30.2156	-72.68414	In Water	CTD Data back	
03/07/16	21:52	30.29136	-72.68412	In Water	Triaxus Issues	Triaxus will not go above 100 m momentarily
03/08/16	0:16	30.57038	-72.66159	In Water	Triaxus lost coms	
03/08/16	0:28	30.59403	-72.65922	In Water	Triaxus coms back on	
03/08/16	3:13	30.95241	-72.64732	In Water	New file started	
03/08/16	9:14	31.69994	-72.53372	In Water	New file started	
03/08/16	16:50	32.66539	-72.39805	In Water	New file started- Switching valve ON	Possible valve failure
03/08/16	17:04	32.69416	-72.39445	In Water	Starting tow yo (5-200 m)	
03/08/16	18:59	32.91546	-72.38841	In Water	Stopped Logging	
03/08/16	19:00	32.91576	-72.38854	On Deck	Triaxus Recovered	
03/08/16	19:41	32.9217	-72.40869	On Deck	Deck Test Started	Removed valve- Bag directly on inlet
03/08/16	20:06	32.92357	-72.42501	On Deck	Deck Test Stopped	
03/08/16	20:13	32.92421	-72.42979	On Deck	Calibration Started- 3_8_3:13	Bag directly on inlet
03/08/16	20:17	32.92544	-72.43324	In Water	Triaxus in Water	
03/08/16	23:08	33.23584	-72.39896	In Water	Triaxus Issues - Stopped Logging	
03/08/16	23:10	33.23762	-72.39906	On Deck	Triaxus Recovered	
03/09/16	0:35	33.30731	-72.44251	On Deck	UMS Powered Up- Started Logging	
03/09/16	0:38	33.30821	-72.44533	In Water	Triaxus in Water- Calibration- 3_8_7:35	Bag directly on inlet
03/09/16	0:53	33.32947	-72.45503	In Water	Starting tow yo (5-200 m)	
03/09/16	2:27	33.53418	-72.41962	In Water	Stopped Logging- Bag empty	
03/09/16	2:33	33.53789	-72.42159	On Deck	Triaxus Recovered	
03/09/16	2:40	33.54022	-72.42452	In Water	Triaxus in Water- Started Logging	
03/09/16	2:55	33.55717	-72.42803	In Water	Starting tow yo (5-200 m)	
03/09/16	9:26	34.39789	-72.22476	In Water	New file started	
03/09/16	13:51	35.01348	-72.05816	In Water	Stopped Logging	
03/09/16	13:56	35.01518	-72.06029	On Deck	Triaxus Recovered	
03/09/16	15:04	35.01791	-72.06384	In Water	Triaxus in Water-	Bag directly on inlet

					Calibration- 3_9	
03/09/16	15:18	35.03977	-72.06605	In Water	Starting tow yo (5-200 m)	
03/09/16	18:16	35.52553	-72.02139	In Water	Bag empty	
03/09/16	18:47	35.60425	-72.01397	On Deck	Triaxus Recovered - Stopped logging	
03/09/16	19:14	35.63372	-72.01366	On Deck	UMS Powered Up- Started Logging	Go Pro Dive
03/09/16	19:16	35.63593	-72.01375	In Water	Triaxus in Water	
03/09/16	19:18	35.63814	-72.01377	In Water	Starting tow yo (2-50 m)	
03/09/16	19:49	35.68538	-72.01269	On Deck	Triaxus Recovered - Stopped logging	Go Pro removed
03/09/16	19:58	35.69425	-72.01383	On Deck	Started logging	
03/09/16	20:01	35.69722	-72.01418	In Water	Triaxus in Water	
03/09/16	20:13	35.71862	-72.01224	In Water	Starting tow yo (5-200 m)	
03/09/16	20:49	35.81797	-72.00021	In Water	Triaxus lost coms	
03/09/16	21:04	35.85179	-71.99809	In Water	Stopped Logging	
03/09/16	21:17	35.8709	-71.99951	On Deck	Triaxus Recovered	Replaced cables on Triaxus
03/10/16	2:51	36.65381	-71.84484	In Water	Triaxus in Water	
03/10/16	2:53	36.65461	-71.84513	In Water	Started Logging	
03/10/16	3:05	36.67263	-71.8437	In Water	Starting tow yo (5-200 m)	
03/10/16	6:15	37.02813	-71.77496	On Deck	Triaxus Recovered for CTD, stopped logging	
03/10/16	8:18	37.00979	-71.77291	In Water	Triaxus in Water	
03/10/16	8:22	37.01029	-71.7736	In Water	Starting tow yo (5-200 m), Start Logging	
03/10/16	12:04	37.37528	-71.68939	In Water	Shallower dives (5-150 m)	
03/10/16	13:32	37.48508	-71.66532	In Water	Stopped Logging	
03/10/16	13:42	37.48311	-71.66107	On Deck	Triaxus Recovered	
03/10/16	22:56	38.93682	-71.51873	In Water	Triaxus in Water- Started Logging	
03/10/16	23:08	38.93886	-71.53471	In Water	Starting tow yo (5-200 m)	
03/11/16	0:23	39.09111	-71.52939	In Water	Shallower dives (5-150 m)	
03/11/16	5:52	39.80995	-71.45585	On Deck	Triaxus Recovered - Stopped logging	

03/11/16	20:06	41.58666	-71.41112	On Deck	Arrive at Narragansett, RI	

Table A2. The timeline of events for EN602.

Date (GMT)	Time (GMT)	Latitude	Longitude	Triaxus Status	Event	Notes
07/06/17	16:00	30.357	-89.0936	In Water	Triaxus dunk test with UMS	
07/07/17	14:10	30.3568	-89.0933	On Deck	Left Gulfport, MS	
07/08/17	0:09	28.7957	-88.3988	On Deck	UMS Powered Up for deployment	
07/08/17	1:15	28.7285	-88.3833	In Water	Triaxus in Water- Started Logging	
07/08/17	1:23	28.7386	-88.3889	In Water	Triaxus weak link broke - floating free	
07/08/17	1:57	28.7365	-88.3849	On Deck	Triaxus Recovered	
07/08/17	5:05	28.7681	-88.3769	In Water	Triaxus in Water	
07/08/17	5:46	28.8357	-88.3743	In Water	Started Logging	
07/08/17	9:29	28.6704	-88.1726	In Water	Begin 'mowing the lawn' over Dauphine Dome	
07/08/17	12:41	28.6357	-88.2526	In Water	New file started	
07/08/17	14:20	28.6174	-88.2952	In Water	Triaxus issues- stopped logging	
07/08/17	15:04	28.6846	-88.3058	On Deck	Triaxus Recovered	
07/08/17	18:17	28.6749	-88.3136	On Deck	Added Switching Valve and coil	88 Second Delay with coil
07/08/17	18:52	28.6852	-88.3101	In Water	Triaxus in Water- Started Logging	UMS deployed with no battery
07/08/17	23:45	28.6986	-89.0428	In Water	Shallower dives (0-50 m)	
07/08/17	23:56	28.6991	-89.0673	In Water	UMS turbo & transpector powered down	
07/09/17	0:00	28.6994	-89.0762	In Water	Began to recover Triaxus, but no issues were found	
07/09/17	0:28	28.6973	-89.1141	In Water	UMS Power Cycled	
07/09/17	1:05	28.6869	-89.1929	In Water	Started Logging	

07/09/17	2:47	28.5811	-89.4199	In Water	UMS issues - UMS Power Cycled (Stopped Logging)	
07/09/17	3:00	28.5697	-89.4487	In Water	New file started	
07/09/17	5:07	28.4025	-89.6989	In Water	UMS issues - UMS Power Cycled (Stopped Logging)	
07/09/17	5:17	28.3912	-89.7193	In Water	Started Logging	
07/09/17	7:19	28.2739	-89.7368	In Water	Deeper dives (5-200 m)	
07/09/17	8:19	28.2313	-89.5778	In Water	Triaxus issues	
07/09/17	8:41	28.2154	-89.5174	In Water	Triaxus Recovered- Stopped Logging	
07/09/17	11:20	28.1386	-89.0013	In Water	Triaxus in Water	
07/09/17	11:23	28.1386	-88.9987	In Water	Started Logging	
07/09/17	11:45	28.1432	-88.9417	In Water	Triaxus coms lost (Stopped logging)	
07/09/17	11:50	28.1446	-88.9281	On Deck	Triaxus Recovered	
07/09/17	15:25	28.1327	-88.4159	In Water	Triaxus in Water- Started Logging	
07/09/17	16:39	28.1664	-88.2435	In Water	Triaxus coms lost (Stopped logging)	
07/09/17	17:13	28.179	-88.1766	On Deck	Triaxus Recovered	Heat sink installed on Triaxus
07/10/17	5:46	26.8835	-86.1676	In Water	Triaxus in Water	
07/10/17	5:53	26.8587	-86.1401	In Water	Started Logging	
07/10/17	8:09	26.5572	-85.8225	In Water	Calibration Started - 7_10	(No S or T recorded)
07/10/17	9:11	26.4225	-85.6674	In Water	Triaxus coms lost (Stopped logging)	
07/10/17	9:30	26.381	-85.6214	In Water	Triaxus weak link broke - floating free	
07/10/17	10:13	26.3665	-85.6211	On Deck	Triaxus Recovered	New battery bulkhead connector
07/12/17	0:45	26.1325	-80.0215	Being Repaired	UMS Powered On for Deck Valve Test	
07/12/17	5:23	26.0242	-80.0681	Being Repaired	UMS Deck Test Stopped	Shortened tubing- 41 second delay
07/12/17	12:53	27.3775	-79.4401	On Deck	UMS Powered Up for	Quick Valve test was

					deployment	completed
07/12/17	15:17	27.7171	-79.2155	On Deck	UMS Power Cycled	
07/12/17	15:35	27.7185	-79.213	In Water	Triaxus in Water- Started Logging	
07/12/17	17:17	27.7155	-78.9602	In Water	Triaxus Shut Down	
07/12/17	17:23	27.7161	-78.9473	In Water	Triaxus rebooted and UMS still logging	
07/12/17	17:44	27.7179	-78.9062	In Water	At depth calibration started	Calibrations occurring at 125 m
07/12/17	17:55	27.7184	-78.879	In Water	Calibration Stopped	S=36.06 T=21.5
07/12/17	18:28	27.7167	-78.796	In Water	At depth calibration started	
07/12/17	18:39	27.7161	-78.768	In Water	Calibration Stopped	
07/12/17	19:10	27.7166	-78.6889	In Water	At depth calibration started	
07/12/17	19:22	27.7179	-78.659	In Water	Calibration Stopped	
07/12/17	19:56	27.7205	-78.5759	In Water	At depth calibration started	
07/12/17	20:07	27.721	-78.5495	In Water	Calibration Stopped	
07/12/17	20:44	27.724	-78.4606	In Water	At depth calibration started	
07/12/17	20:55	27.7255	-78.4349	In Water	Calibration Stopped	
07/12/17	21:28	27.7313	-78.3612	In Water	At depth calibration started	
07/12/17	21:39	27.7336	-78.3336	In Water	Calibration Stopped	
07/12/17	22:13	27.7417	-78.2574	In Water	At depth calibration started	
07/12/17	22:24	27.7433	-78.2336	In Water	Calibration Stopped	
07/12/17	22:49	27.7438	-78.1807	In Water	Lost coms with Triaxus- Stopped logging	
07/12/17	23:14	27.7472	-78.1523	On Deck	Triaxus Recovered	
07/13/17	1:05	27.7483	-77.9018	In Water	Triaxus in Water with new cover	Seasave file on CDT
07/13/17	4:23	27.7153	-77.4331	In Water	Calibration Started - 7_13	S=36.06 T=21.5
07/13/17	8:08	27.7261	-76.8808	In Water	Calibration 7_13 stopped, New file started	Seasave file back on EDT
07/13/17	14:08	27.7309	-75.9518	In Water	New file started	
07/13/17	20:24	27.7363	-74.9416	In Water	New file started	
07/14/17	2:37	27.7616	-73.8792	In Water	Lost coms with Triaxus- Stopped logging	

07/14/17	2:44	27.7616	-73.8593	In Water	New file started	
07/14/17	9:02	27.7453	-72.809	In Water	New file started	
07/14/17	12:22	28.1096	-72.6174	In Water	Changed maximum depth to 150 m	
07/14/17	15:31	28.5738	-72.6056	In Water	New file started	
07/14/17	18:30	29.0016	-72.567	In Water	UMS coms went out and returned	
07/14/17	18:36	29.0158	-72.5654	In Water	UMS turbo & transpector powered down	
07/14/17	18:42	29.0274	-72.5642	On Deck	Triaxus Recovered	
07/14/17	19:37	29.0397	-72.5478	On Deck	CTD Cast 1	
07/14/17	21:35	29.0368	-72.5482	On Deck	UMS power cable issue	
07/15/17	1:09	29.5151	-72.5032	In Water	Triaxus in Water	
07/15/17	1:13	29.5192	-72.5032	In Water	New file started	
07/15/17	5:09	30.085	-72.4507	In Water	Calibration Started - 7_15	S=36.64 T=23.1
07/15/17	7:42	30.4732	-72.4148	In Water	Calibration 7_15 Stopped	
07/15/17	8:08	30.539	-72.4077	In Water	New file started	
07/15/17	14:53	31.5491	-72.3271	In Water	New file started	
07/15/17	22:24	32.7047	-72.231	On Deck	Triaxus Recovered for CTD, stopped logging	
07/15/17	23:07	32.7074	-72.2295	On Deck	UMS Deck Calibration	S=36.06 T=21.5 Bag directly on inlet
07/15/17	23:18	32.7073	-72.2293	On Deck	CTD Cast 2	
07/16/17	2:00	32.6903	-72.2359	On Deck	Stopped Deck Calibration	
07/16/17	2:42	32.6924	-72.2425	In Water	Triaxus in Water- Started Logging	
07/16/17	5:22	33.08	-72.2027	In Water	Calibration Started - 7_16	S=36.64 T=23.1
07/16/17	7:46	33.4008	-72.1489	In Water	Calibration 7_16 Stopped	
07/16/17	9:04	33.5695	-72.1252	In Water	New file started	
07/16/17	16:15	34.6434	-71.9854	In Water	New file started	
07/16/17	22:36	35.6259	-71.9189	In Water	New file started	
07/17/17	4:07	36.4883	-71.8326	In Water	New file started	
07/17/17	10:53	37.6085	-71.7262	In Water	New file started	
07/17/17	16:40	38.4739	-71.6398	On Deck	Triaxus Recovered for CTD,	

					stopped logging	
07/17/17	16:51	38.4743	-71.6361	On Deck	CTD Cast 3	
07/17/17	17:51	38.4851	-71.6368	In Water	Triaxus in Water	
07/17/17	17:54	38.4876	-71.6368	In Water	New file started	
07/18/17	2:08	39.7293	-71.5184	In Water	Calibration Started - 7_17	(No S or T recorded)
07/18/17	3:29	39.9068	-71.4849	On Deck	Triaxus Recovered, Still logging calibration	
07/18/17	4:19	40.0479	-71.476	On Deck	Calibration 7_17 Stopped	
07/18/17	13:56	41.494	-71.4187	On Deck	Arrive at GSO	

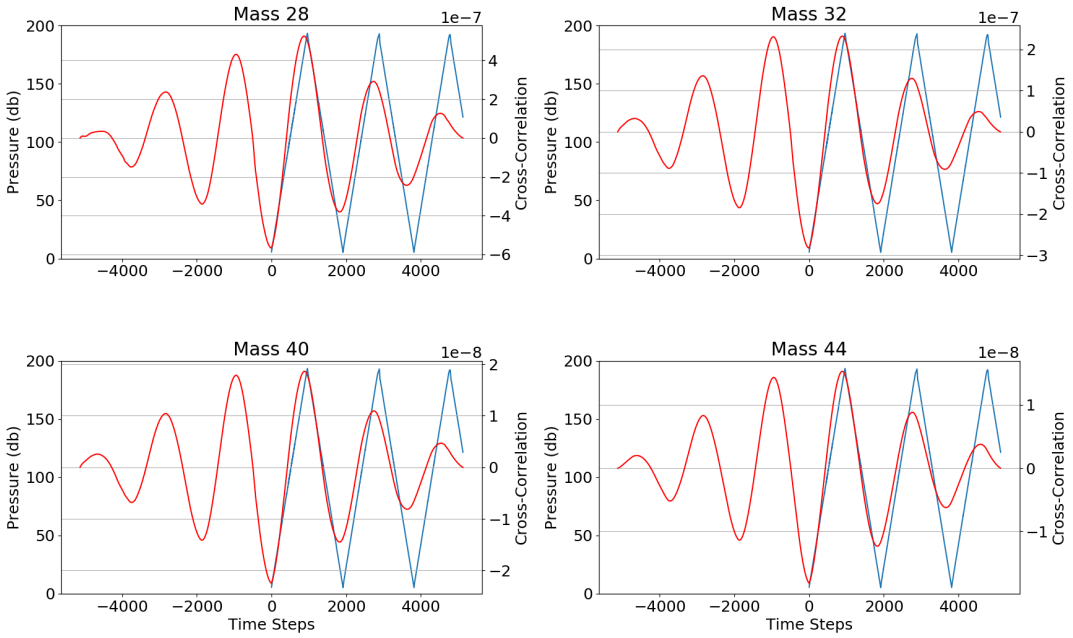

Figure A1. The serial cross correlation (red line), plotted in time with the hydrostatic pressure (blue line) during a calibration tow on EN575.

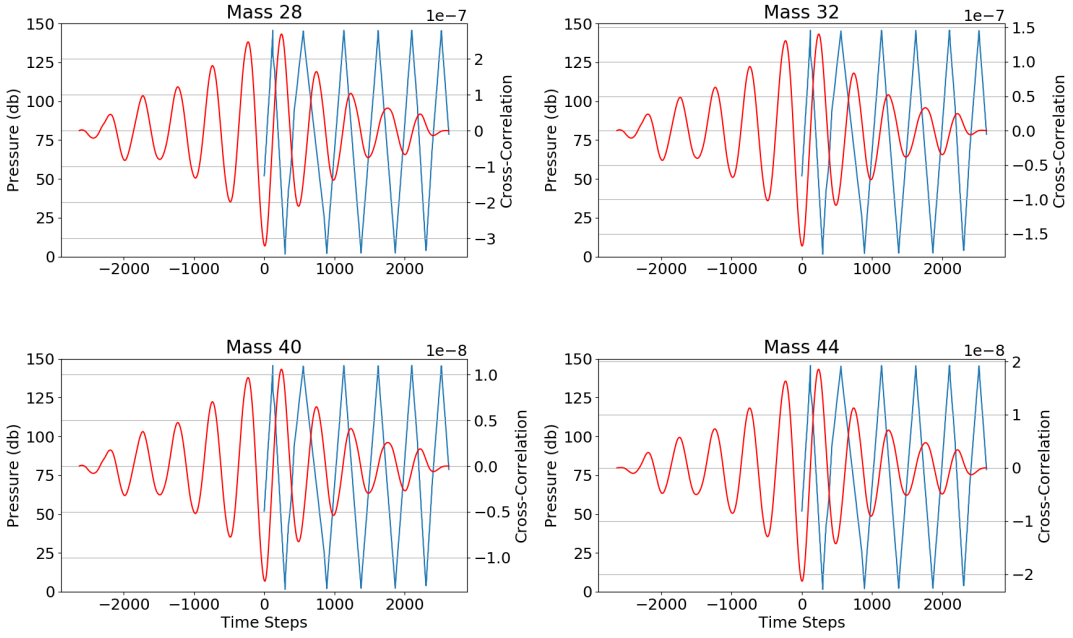

Figure A2. The serial cross correlation (red line), plotted in time with the hydrostatic pressure (blue line) during a calibration tow on EN602.

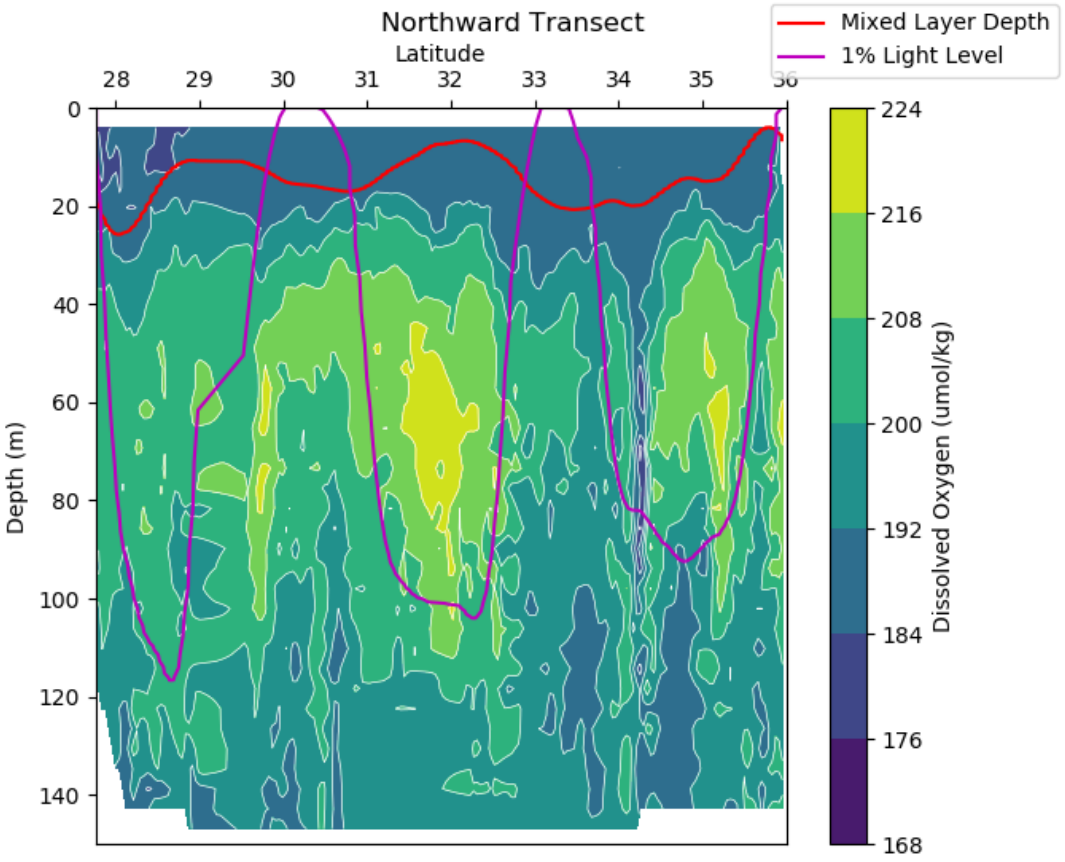

Figure A3. The northward transect of dissolved oxygen concentrations measured from the Seabird 43 attached to the Triaxus on EN602. Sampling at the surface of the ocean would not capture the structure seen through the mixed layer depth (red line) and photic zone (purple line). The large amount of oxygen structure in the top 150 meters highlights the potential of UMS measurements to resolve upper ocean structure for many dissolved gases.

BIBLIOGRAPHY

Akaike, H. (1974). A new look at the statistical model identification. *IEEE Transactions on Automatic Control*, *19*(6), 716–723. https://doi.org/10.1109/TAC.1974.1100705

Bell, R. J., Short, R. T., van Amerom, F. H. W., & Byrne, R. H. (2007). Calibration of an In Situ Membrane Inlet Mass Spectrometer for Measurements of Dissolved Gases and Volatile Organics in Seawater. *Environmental Science & Technology*, *41*(23), 8123–8128. https://doi.org/10.1021/es070905d

Bell, R. J., Savidge, W. B., Toler, S. K., Byrne, R. H., & Short, R. T. (2012). In situ determination of porewater gases by underwater flow-through membrane inlet mass spectrometry. *Limnology and Oceanography-Methods*, *10*, 117–128. https://doi.org/10.4319/lom.2012.10.117

Brainerd, K. E., & Gregg, M. C. (1995). Surface mixed and mixing layer depths. *Deep Sea Research Part I: Oceanographic Research Papers*, *42*(9), 1521–1543. https://doi.org/10.1016/0967-0637(95)00068-H

Brennwald, M. S., Schmidt, M., Oser, J., & Kipfer, R. (2016). A Portable and Autonomous Mass Spectrometric System for On-Site Environmental Gas Analysis. *Environmental Science & Technology*, *50*(24), 13455–13463. https://doi.org/10.1021/acs.est.6b03669

Burnham, K. P., & Anderson, D. R. (2004). Multimodel Inference: Understanding AIC and BIC in Model Selection. *Sociological Methods & Research*, *33*(2), 261–304. https://doi.org/10.1177/0049124104268644

Ducklow, H. W., & Doney, S. C. (2013). What Is the Metabolic State of the Oligotrophic Ocean? A Debate. *Annual Review of Marine Science*, *5*(1), 525–533. https://doi.org/10.1146/annurev-marine-121211-172331

Ferrón, S., del Valle, D. A., Björkman, K. M., Quay, P. D., Church, M. J., & Karl, D. M. (2016). Application of membrane inlet mass spectrometry to measure aquatic gross primary production by the 18O in vitro method. *Limnology and Oceanography: Methods*, *14*(9), 610–622. https://doi.org/10.1002/lom3.10116

Futó, I., & Degn, H. (1994). Effect of sample pressure on membrane inlet mass spectrometry. *Analytica Chimica Acta*, *294*(2), 177–184. https://doi.org/10.1016/0003-2670(94)80192-4

Glover, D. M., Jenkins, W. J., & Doney, S. C. (2011). *Modeling methods for marine science*. Cambridge ; New York: Cambridge University Press.

Hill, T., & Lewicki, P. (2006). *Statistics: methods and applications: a comprehensive reference for science, industry, and data mining*. Tulsa, OK: StatSoft.

Hoegh-Guldberg, O., & Bruno, J. F. (2010). The Impact of Climate Change on the World's Marine Ecosystems. *Science*, *328*(5985), 1523–1528. https://doi.org/10.1126/science.1189930

James, G., Witten, D., Hastie, T., & Tibshirani, R. (2013). *An Introduction to Statistical Learning* (Vol. 103). New York, NY: Springer New York. https://doi.org/10.1007/978-1-4614-7138-7

Janfelt, C., Lauritsen, F. R., Toler, S. K., Bell, R. J., & Short, R. T. (2007). Method for Quantification of Chemicals in a Pollution Plume Using a Moving Membrane-Based Sensor Exemplified by Mass Spectrometry. *Analytical Chemistry*, *79*(14), 5336–5342. https://doi.org/10.1021/ac070408f

Jolliffe, I. T. (1986). Principal Component Analysis and Factor Analysis. In *Principal Component Analysis* (pp. 115–128). Springer, New York, NY. https://doi.org/10.1007/978-1-4757-1904-8_7

Keeling, R. F., Körtzinger, A., & Gruber, N. (2009, December 14). Ocean Deoxygenation in a Warming World [review-article]. Retrieved February 17, 2017, from http://www.annualreviews.org.uri.idm.oclc.org/doi/10.1146/annurev.marine.010908.163855

Lee, W. S., Yeo, K. S., Andriyana, A., Shee, Y. G., & Mahamd Adikan, F. R. (2016). Effect of cyclic compression and curing agent concentration on the stabilization of mechanical properties of PDMS elastomer. *Materials & Design*, *96*(Supplement C), 470–475. https://doi.org/10.1016/j.matdes.2016.02.049

McMurtry, G. M., Kolotyrkina, I. Y., Lee, J. S., & Kim, K. H. (2012). Underwater mass spectrometers for in situ monitoring of dissolved gases and volatile organic compounds in deep ocean and coastal environments. In *2012 Oceans - Yeosu* (pp. 1–6). https://doi.org/10.1109/OCEANS-Yeosu.2012.6263597

Miles, E. L. (2009, October 15). On the Increasing Vulnerability of the World Ocean to Multiple Stresses [review-article]. Retrieved February 13, 2017, from http://www.annualreviews.org/doi/10.1146/annurev.environ.33.041707.110117

Moore, C. M., Mills, M. M., Arrigo, K. R., Berman-Frank, I., Bopp, L., Boyd, P. W., et al. (2013). Processes and patterns of oceanic nutrient limitation. *Nature Geoscience*, *6*(9), 701–710. https://doi.org/10.1038/ngeo1765

Rabiner, L. R., & Gold, B. (1975). *Theory and application of digital signal processing*. Englewood Cliffs, N.J: Prentice-Hall.

Reuer, M. K., Barnett, B. A., Bender, M. L., Falkowski, P. G., & Hendricks, M. B. (2007). New estimates of Southern Ocean biological production rates from

O2/Ar ratios and the triple isotope composition of O2. *Deep Sea Research Part I: Oceanographic Research Papers*, *54*(6), 951–974. https://doi.org/10.1016/j.dsr.2007.02.007

Servén, D. (2018). *pyGAM: Generalized Additive Models in Python*. Python. Retrieved from https://github.com/dswah/pyGAM (Original work published January 19, 2017)

Short, R. T., Fries, D. P., Toler, S. K., Lembke, C. E., & Byrne, R. H. (1999). Development of an underwater mass-spectrometry system for in situ chemical analysis. *Measurement Science and Technology*, *10*(12), 1195. https://doi.org/10.1088/0957-0233/10/12/311

Sommer, S., Schmidt, M., & Linke, P. (2015). Continuous inline mapping of a dissolved methane plume at a blowout site in the Central North Sea UK using a membrane inlet mass spectrometer – Water column stratification impedes immediate methane release into the atmosphere. *Marine and Petroleum Geology*, *68*, *Part B*, 766–775. https://doi.org/10.1016/j.marpetgeo.2015.08.020

Stone, M. (1977). An Asymptotic Equivalence of Choice of Model by Cross-Validation and Akaike's Criterion. *Journal of the Royal Statistical Society. Series B (Methodological)*, *39*(1), 44–47.

Sysoev, A. A. (2000). A Mathematical Model for Kinetic Study of Analyte Permeation from Both Liquid and Gas Phases through Hollow Fiber Membranes into Vacuum. *Analytical Chemistry*, *72*(17), 4221–4229. https://doi.org/10.1021/ac991388n

Talley, L. D. (2011). *Descriptive physical oceanography an introduction*. Amsterdam; Boston: Academic Press. Retrieved from http://www.sciencedirect.com/science/book/9780750645522